Elastic-skinned gravity currents

Anja Slim

1 Introduction

We investigate a thin layer of very viscous fluid that flows down a slope due to gravity. However, instead of the usual free surface, the fluid is covered by an elastic plate. This allows for interesting wrinkling patterns to develop on the fluid surface.

One motivation for considering this problem is lava flows. A pahoehoe lava flow could be crudely considered an elastic-skinned gravity current. As a flow advances, it solidifies at the surface, forming a crust whilst remaining molten in the interior. An interesting aspect of these flows is the surface features that can be produced. One form, known as 'ropy' pahoehoe lava, is shown in figure 1(a). The traditional explanation for this phenomena is that the fluid beneath the crust pulls at it, and drags it into folds (see Ollier [2]). However, Fink and Fletcher [3] observed that the buckling was most prominent downstream of a constriction or a sudden decrease in bottom slope. They proposed that the explanation for buckling is that faster fluid pushes crust above it into crust above slower fluid. The resulting compression causes buckling. They also modelled this assuming the lava was semi-infinite and with a depth dependent viscosity.

A second motivation comes from experiments done by Clayton and Belmonte [1] with micellar fluid. Instead of mixing the two components of micellar fluid (aqueous solutions of surfactant and organic salt), they pumped one into the other. This resulted in a gravity current forming with an elastic interface between the two components. Clayton and Belmonte performed experiments on a slope, and observed fingering similar to that seen in a viscous fluid (see, for example, Huppert [4]). However when the volume flux was reduced during an experiment, buckling was observed along the fingers, as seen in figure 1(b).

The aim of this report is to begin to understand elastic-skinned gravity currents and buckling on their surfaces. It is organized as follows. In §2 we give a brief overview of previous work done on elastic-skinned gravity currents and general problems in hydro-elasticity. In §3 we outline some simple experiments and results. These experiments were performed to obtain a qualitative appreciation of the main features of these gravity currents. In §4 we formulate the governing system of equations. In §5 we present some preliminary analysis on three problems related to the currents. The first considers how the fluid influences buckling, the second considers how fluid traction at the base of the elastic plate can induce buckling and the final problem begins to combine these aspects to model the gravity current of the experiments in §3. Finally, §6 presents some conclusions and discusses future work.
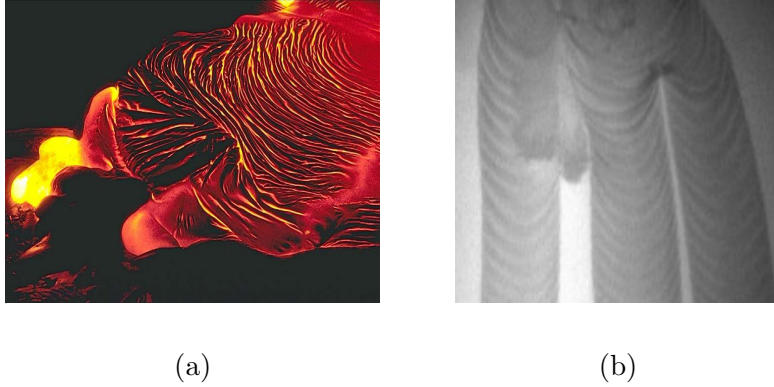
(a)   (b)

Figure 1: (a) Ropy pahoehoe lava. (b) Wrinkling observed on a gravity current finger between aqueous surfactant and organic salt solutions. *From* Clayton and Belmonte [1].

2 Previous work on hydro-elasticity

There has been much work done on problems of interaction of elastic materials with fluids. Major areas of application are to blood flow, flutter and drag reduction. Arteries are modelled as elastic-walled tubes filled with fluid, see for example Grotberg and Jensen [5]. Flutter usually refers to high Reynolds number flow over thin objects which causes vibrations, for example on aeroplanes (see, for example, Gee [6]). The application to drag reduction comes from an observation (for example Benjamin [7]) that replacing part of a solid wall by an elastic membrane increases the background velocity at which a turbulent boundary layer forms. Geophysical applications include modelling wave propagation through ice sheets on the ocean surface as waves in an elastic plate above an inviscid fluid (for example Chakrabarti et al. [8]). A further geophysical application is to magma flow through elastic-walled volcanic conduits (Balmforth et al. 2004 [9]).

To our knowledge, the only work that has investigated elastic-skinned gravity currents is the recent work of Hosoi and Mahadevan [10]. They studied the two-dimensional 'peeling' problem associated with fluid forced between an elastic plate and a rigid base, with which the plate is initially in contact. They model this system using the lubrication equation coupled with a linear plate equation.

3 Experiments

To investigate the behaviour of elastic-skinned gravity currents, we carried out experiments with a set-up as shown in figure 2. An elastic plate, either cling-wrap or exercise stretch band, was clamped to a rigid base and corn syrup was pumped between them.

The experiments were preliminary, although some qualitative observations can be made. Figure 3(a) shows the system with no initial slack (the plate was initially flat on the rigid base). Two important points about this configuration are that no wrinkles are visible and that the black line, which was perpendicular to the clamped edges before the fluid was pumped in, has not perceptively deformed. Figure 3(b) shows the system with an
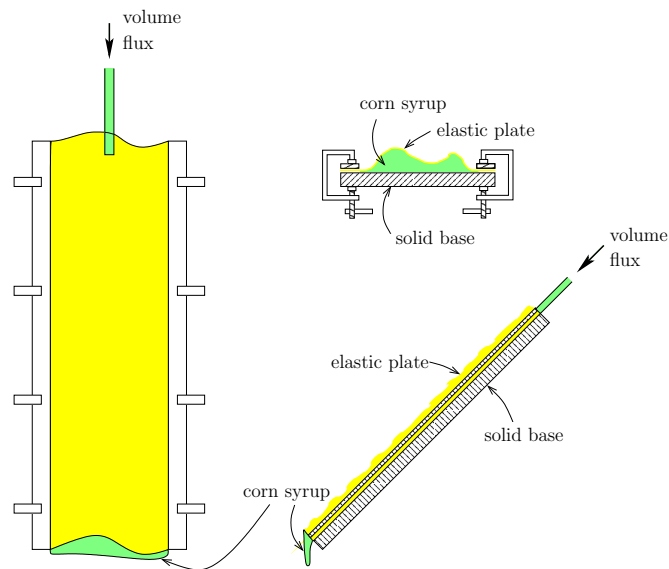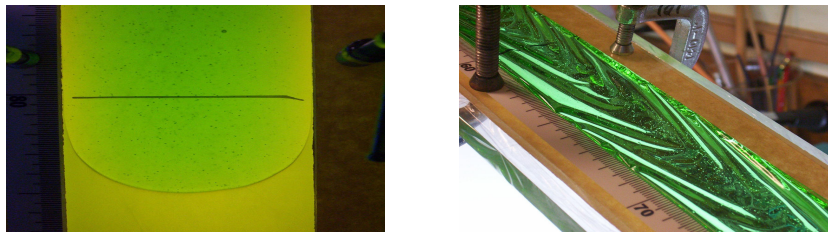
Figure 2: The experimental arrangement.

initial slack and with a fluid volume insufficient to fill it. Wrinkles are prominent and are clearly oriented downstream. Some other general points are: for a given flux and slack, the wavelength of the wrinkles increases with increasing width and increasing angle of slope; and the wavelength increases as the material becomes stiffer.[1]

(a)

(b)

Figure 3: (a) Advancing front of the fluid beneath the elastic plate (exercise stretch band) for a case with no initial slack. No wrinkles are apparent. (b) A case with initial slack and clear wrinkles in the elastic plate (cling wrap).

---

[1]The wavelength was also observed to increase downstream from the source, but this is possibly an artefact of the way fluid was injected.
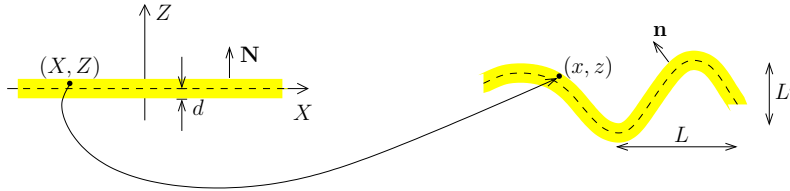
Figure 4: The elastic plate in its (left) undeformed and (right) deformed configuration. The undeformed coordinates are (X, Z) and the deformed (x, z). The horizontal length scale for the deformation of the plate is L and the vertical L'. The half-thickness of the plate is d.

4 Governing equations

There are three aspects of the configuration that need to be modelled: the elastic plate, the viscous fluid and the interaction between the two. We present equations for these in §§4.2, 4.3 and 4.4 respectively; together with boundary conditions on the plate and the fluid in §4.5. For the elastic plate we use the generalized von Kármán plate equations, which are nonlinear and include buckling terms. The fluid is described by the Stokes' equations.

Before presenting the governing equations for each component of the system, we give a derivation of the two-dimensional generalized von Kármán plate equations, to obtain an idea of the conditions under which they may be applied.

4.1 Derivation of the two-dimensional generalized von Kármán equations

The elastic plate is assumed to be very thin compared to the typical plate dimension, hence we derive the generalized two-dimensional von Kármán plate equations via asymptotics. By 'generalized', we refer to the particular form of the equations that have extra terms for in-plane forcings on the top and bottom of the plate: the original von Kármán equations only included normal forcing (see Yu [11]).

The usual method of derivation is from force balances. For example, Fung [12] derives the original von Kármán equations and Timoshenko [13] a generalized form with in-plane forcings on the plate (although some terms that are included in Yu and the derivation we present are not included there). An alternative method of derivation is a variational approach. For example, Landau and Lifschitz [14] derive the original equations and Yu the generalized.

Ciarlet [15] gave an asymptotic derivation for the original von Kármán equations. This was extended by various authors, for example, Millet et al. [16], to the generalized equations. In both cases, the authors assumed 'dead' loads: forcings that are independent of the deformation of the plate. Here we give a very similar derivation: our scalings are slightly different, but the expansion is essentially the same. We are also interested in forcings that do depend on the deformation of the plate to enable the coupling of the plate and the fluid.

We first give a brief overview of non-linear elasticity, to put our asymptotics into context. The system we are considering is shown in figure 4.

We may think of an elastic plate in two different coordinate systems. One is the undeformed, or Lagrangian, system in which everything is referred to the initial configuration

of the plate. The other is the deformed, or Eulerian, system in which things are referred to their current configuration. In two dimensions, the undeformed configuration is given by $\mathbf{X} = (X, Z)$ and the deformed configuration by $\mathbf{x} = (x, z)$ with

$$x = X + \xi(X, Z), \qquad z = Z + \zeta(X, Z), \tag{1}$$

where $\boldsymbol{\xi} = (\xi, \zeta)$ is the displacement.

The deformation gradient tensor converts between the two coordinate systems

$$F_{ij} = \partial x_i / \partial X_j.$$

The equation for conservation of momentum applies in the interior of the plate. From a fluid dynamics perspective, it may be considered most naturally in the deformed configuration and is given by

$$\nabla_{\mathbf{x}} \cdot \boldsymbol{\sigma} = 0, \tag{2}$$

where $\nabla_{\mathbf{x}} \cdot$ is the divergence and $\boldsymbol{\sigma}$ is the Cauchy stress tensor, both in the deformed coordinates. Throughout the report, subscripts $\mathbf{x}$ and $\mathbf{X}$ emphasize quantities in the deformed and undeformed configuration respectively. This equation assumes no body forces act on the plate and that the plate is in equilibrium. In our fluid–plate interaction problem elastic waves are fast compared to the viscous fluid flow and hence the plate at any instant may be assumed in equilibrium.

The boundary conditions on the plate are

$$\boldsymbol{\sigma} \cdot \mathbf{n} = \mathbf{t_x} \tag{3}$$

on the upper and lower surfaces of the plate, $z = \pm d + \zeta(X, \pm d)$, where d is the constant half-thickness of the plate, $\mathbf{n}$ is the normal to the plate and $\mathbf{t_x}$ is the surface traction imposed on it.

It is easier to derive the plate equations in the undeformed configuration because then the normal is simpler and we do not have to keep track of the location of the boundary of the plate. Although, in order to couple the plate equations with the fluid, we ultimately convert the derived equations back into the deformed coordinate system. Using the relation (see, for example, Antman [17] pg. 405, 406)

$$\boldsymbol{\sigma} = J^{-1} \mathbf{F} \boldsymbol{\Sigma} \mathbf{F}^T,$$

where $\boldsymbol{\Sigma}$ is the second Piola–Kirchoff stress tensor for the stress referred to the undeformed configuration, and $J = \det \boldsymbol{F}$, we translate (2) and (3) into the undeformed coordinate system as

$$\nabla_{\mathbf{X}} \cdot \boldsymbol{\Sigma} \mathbf{F}^T = 0, \tag{4}$$

$$\mathbf{F} \boldsymbol{\Sigma} \cdot \mathbf{N} = \sqrt{(1 + \xi_{,X})^2 + \zeta_{,X}^2} \, \mathbf{t_x}, \tag{5}$$

where $\mathbf{N}$ is the normal in the undeformed configuration, $\mathbf{t_x}$ is still the traction in the deformed configuration[2] and the boundary condition is now at $Z = \pm d$. The ",·" subscript

---

[2]Note that this forcing still depends on $\boldsymbol{\xi}$. This means it should also be expanded and is something that still needs to be cleaned up.

refers to derivatives, a notation we use throughout the report. We introduce this notation to avoid confusion because later we will use plain subscripts, such as Σ_{XX}, to denote components of tensors.

The stress tensor, $\boldsymbol{\Sigma}$, may be related to the strain tensor, $\mathbf{E}$, through the linear, isotropic constitutive relation

$$\boldsymbol{\Sigma} = 2\tilde{\mu}\mathbf{E} + \tilde{\lambda}E_{kk}\mathbf{I}, \tag{6}$$

where $\tilde{\lambda}$, $\tilde{\mu}$ are Lamé constants and $\mathbf{E}$ is the non-linear strain tensor given by

$$E_{ij} = \frac{1}{2}\left(\frac{\partial \xi_i}{\partial X_j} + \frac{\partial \xi_j}{\partial X_i} + \frac{\partial \xi_k}{\partial X_i}\frac{\partial \xi_k}{\partial X_j}\right). \tag{7}$$

Note that using a linear constitutive model but non-linear strain is consistent provided that the strains are small (Stoker [18]).

We now look for solutions of the system (4) and (5) for which $\epsilon = L'/L \ll 1$, where L' is a length-scale associated with the out-of-plane displacements and L is a horizontal length-scale. Setting $L' = d$ is identical to Ciarlet [15] and Millet et al. [16]. We use the scaling

$$\xi = \epsilon L'\hat{\xi}, \quad \zeta = L'\hat{\zeta}, \quad X = L\hat{X}, \quad Z = \delta L'\hat{Z}, \quad t_x = \tilde{\mu}\epsilon^3\hat{t}_x, \quad t_z = \tilde{\mu}\epsilon^4\hat{t}_z, \tag{8}$$

where $\delta = d/L'$ and ϵ is much less than δ in a way made precise below. These assumptions are consistent with the scalings suggested in our experiments of §3. Scaling the momentum equation (4), neglecting hats, then gives

$$\left(\Sigma_{XX} + \epsilon^2\xi_{,X}\Sigma_{XX} + \frac{1}{\delta}\epsilon\xi_{,Z}\Sigma_{XZ}\right)_{,X} + \left(\frac{1}{\epsilon}\frac{1}{\delta}\Sigma_{XZ} + \frac{1}{\delta^2}\xi_{,Z}\Sigma_{ZZ} + \epsilon\frac{1}{\delta}\xi_{,X}\Sigma_{XZ}\right)_{,Z} = 0 \tag{9}$$

$$\left(\zeta_{,X}\Sigma_{XX} + \epsilon\Sigma_{XZ} + \epsilon\frac{1}{\delta}\zeta_{,Z}\Sigma_{XZ}\right)_{,X} + \left(\frac{1}{\delta}\Sigma_{ZZ} + \frac{1}{\delta^2}\zeta_{,Z}\Sigma_{ZZ} + \epsilon\frac{1}{\delta}\zeta_{,X}\Sigma_{XZ}\right)_{,Z} = 0, \tag{10}$$

and the boundary conditions (5) gives

$$\epsilon^{-1}\Sigma_{XZ} + \frac{1}{\delta}\xi_{,Z}\Sigma_{ZZ} + \epsilon\xi_{,X}\Sigma_{XZ} = \begin{cases} 0 & \text{on } Z = 1 \\ \tilde{\mu}\epsilon^2 t_x & \text{on } Z = -1 \end{cases}, \tag{11}$$

$$\left(1 + \frac{1}{\delta}\zeta_{,Z}\right)\Sigma_{ZZ} + \epsilon\zeta_{,X}\Sigma_{XZ} = \begin{cases} 0 & \text{on } Z = 1 \\ \tilde{\mu}\epsilon^4 t_z & \text{on } Z = -1 \end{cases}. \tag{12}$$

Into these equations, we substitute the formal expansion,

$$\xi = \xi_0(\mathbf{X}) + \epsilon^2\xi_2(\mathbf{X}) + \epsilon^4\xi_4(\mathbf{X}) + \cdots, \quad \zeta = \zeta_0(\mathbf{X}) + \epsilon^2\zeta_2(\mathbf{X}) + \epsilon^4\zeta_4(\mathbf{X}) + \cdots,$$

where only even order terms have been included, as odd order ones are irrelevant in the results we present.

186

Expanding **E** in powers of ϵ, from (7) and dropping the hats, gives

$$E_{XX} = E_{XX}^{(0)} + \epsilon^2 E_{XX}^{(2)} + \cdots$$
$$= 0 + \epsilon^2 \left(\xi_{0,X} + \frac{1}{2}\zeta_{0,X}^2 \right) + \cdots$$
$$E_{ZZ} = E_{ZZ}^{(0)} + \epsilon^2 E_{ZZ}^{(2)} + \cdots$$
$$= \left(\delta^{-1}\zeta_{0,Z} + \frac{1}{2}\delta^{-2}\zeta_{0,Z}^2 \right) + \epsilon^2 \left(\delta^{-1}\zeta_{2,Z} + \frac{1}{2}\delta^{-2}\xi_{0,Z}^2 + \delta^{-2}\zeta_{0,Z}\zeta_{2,Z} \right) + \cdots$$

for the normal strain components and

$$E_{XZ} = \epsilon E_{XZ}^{(1)} + \cdots$$
$$= \epsilon \left(\frac{1}{2}\delta^{-1}\xi_{0,Z} + \frac{1}{2}\zeta_{0,X} + \frac{1}{2}\delta^{-1}\zeta_{0,X}\zeta_{0,Z} \right) + \cdots$$

for the shear strain. From these, the stresses may be written, using (6) as

$$\Sigma_{XX}^{(k)} = (\tilde{\lambda} + 2\tilde{\mu})E_{XX}^{(k)} + \tilde{\lambda}E_{ZZ}^{(k)}, \quad \Sigma_{XZ}^{(k)} = 2\tilde{\mu}E_{XZ}^{(k)}, \quad \Sigma_{ZZ}^{(k)} = \tilde{\lambda}E_{XX}^{(k)} + (\tilde{\lambda} + 2\tilde{\mu})E_{ZZ}^{(k)}.$$

We can now begin with the asymptotics.

At order 1, the equations and boundary conditions (9), (11) and (10), (12) imply

$$\Sigma_{ZZ}^{(0)} \left(1 + \delta^{-1}\zeta_{0,Z} \right) = 0, \quad \Sigma_{XZ}^{(1)} + \delta^{-1}\xi_{0,Z}\Sigma_{XX}^{(0)} = 0,$$

respectively. The former of these gives three possible solutions and we choose the physically most meaningful

$$\Sigma_{ZZ}^{(0)} = \zeta_{0,Z} = 0.$$

Hence to leading order the out-of-plane displacement is independent of Z. The second equation then gives

$$\Sigma_{XZ}^{(1)} = 0, \qquad \xi_0(X, Z) = -\delta\zeta_{0,X}Z + \tilde{\xi}_0(X),$$

where $\tilde{\xi}_0(X)$ may be interpreted as the in-plane displacement of the centre-line of the plate.

At order ϵ^2, the equations become

$$\Sigma_{XX,X}^{(2)} + \delta^{-1}\Sigma_{XZ,Z}^{(3)} = 0, \tag{13}$$

subject to $\Sigma_{XZ}^{(3)} = 0$ on $Z = 1$ and $\Sigma_{XZ}^{(3)} = \tilde{\mu}t_z$ on $Z = -1$ from (9) and (11), and from (10) and (12)

$$\Sigma_{ZZ}^{(2)} = 0.$$

This last equation may be solved for ζ_2 to give

$$\zeta_2 = \frac{\tilde{\lambda}}{\tilde{\lambda} + 2\tilde{\mu}} \left(\delta^2 \zeta_{0,XX} \frac{1}{2}Z^2 - \delta\tilde{\xi}_{0,X}Z \right) - \delta \frac{\tilde{\lambda} + \tilde{\mu}}{\tilde{\lambda} + 2\tilde{\mu}}\zeta_{0,X}^2,$$

where constant terms of integration have been neglected because they are not relevant in our derivation. Equation (13) gives

$$\Sigma_{XZ}^{(3)} = -\tilde{\mu}\delta\frac{4(\tilde{\lambda}+\tilde{\mu})}{\tilde{\lambda}+2\tilde{\mu}}\left[-\delta\zeta_{0,XXX}\frac{1}{2}Z^2 + \tilde{\xi}_{0,XX}Z + \frac{1}{2}\left(\zeta_{0,X}^2\right)_X Z\right] + A(X),$$

where $A(X)$ is a constant function (in Z) of integration. $A(X)$ may be eliminated using $\left[\Sigma_{XZ}^{(3)}\right]_{-1}^{1} = -\tilde{\mu}t_x$ from the boundary conditions, to give the first of the generalized von Kármán equations:

$$\frac{8(\tilde{\lambda}+\tilde{\mu})}{\tilde{\lambda}+2\tilde{\mu}}\delta\left[\tilde{\xi}_{0,XX} + \frac{1}{2}\left(\zeta_{0,X}^2\right)_X\right] = t_x. \tag{14}$$

This equation governs the in-plane deformation of the plate. We will also require the solution for $A(X)$, which may be found by taking the sum $\Sigma_{XZ}^{(3)}\big|_{Z=1} + \Sigma_{XZ}^{(3)}\big|_{Z=-1}$ and is

$$2A(X) = \tilde{\mu}t_x - \tilde{\mu}\delta^2\frac{4(\tilde{\lambda}+\tilde{\mu})}{\tilde{\lambda}+2\tilde{\mu}}\zeta_{0,XXX}.$$

At order ϵ^4, equations (10) and (12) combine to give

$$\int_{-1}^{1}\left(\zeta_{0,X}\Sigma_{XX}^{(2)} + \Sigma_{XZ}^{(3)}\right)_X \mathrm{d}Z = -\delta^{-1}\left[\zeta_{0,X}\Sigma_{XZ}^{(3)} + \Sigma_{ZZ}^{(4)}\right]_{-1}^{1} = -\delta^{-1}\tilde{\mu}t_z,$$

from which, provided $\delta^3 \gg \epsilon$, the second generalized von Kármán equation becomes

$$\frac{8(\tilde{\lambda}+\tilde{\mu})}{3(\tilde{\lambda}+2\tilde{\mu})}\delta^3\zeta_{0,XXXX} = -t_z + \frac{8(\tilde{\lambda}+\tilde{\mu})}{\tilde{\lambda}+2\tilde{\mu}}\delta\left(\zeta_{0,X}\tilde{\xi}_{0,X} + \frac{1}{2}\zeta_{0,X}^3\right)_X + \delta t_{x,X}, \tag{15}$$

which governs the out-of-plane flexing of the plate. If $\delta^3 \sim \epsilon$, then the first term, the flexural term, should be neglected and we obtain a membrane model. The previous orders appear to be consistent in the asymptotic expansion provided $\delta^2 \gg \epsilon$.

We now transform equations (14) and (15) back into the deformed coordinate system. From (1) and the scalings (8), we have

$$\frac{\partial}{\partial X} = \frac{\partial}{\partial x} + \mathcal{O}(\epsilon).$$

Hence, by replacing all derivatives in X by derivatives in x, we obtain the generalized von Kármán equations, on rescaling, in the deformed configuration.

We can also calculate the energy density for the elastic plate from the asymptotics. For an elastic body, the energy density becomes

$$\psi = \frac{1}{2}\Sigma_{ij}E_{ij} = \epsilon^4\left[\frac{1}{2}(\tilde{\lambda}+2\tilde{\mu})\left(E_{XX}^{(2)2} + E_{ZZ}^{(2)2}\right) + \tilde{\lambda}E_{XX}^{(2)}E_{ZZ}^{(2)}\right] + \mathcal{O}(\epsilon^6) \tag{16}$$

$$= \epsilon^4\frac{4(\tilde{\lambda}+\tilde{\mu})\tilde{\mu}}{\tilde{\lambda}+2\tilde{\mu}}\left[\frac{1}{3}\delta^2\zeta_{0,XX}^2 + \left(\tilde{\xi}_{0,X} + \frac{1}{2}\zeta_{0,X}^2\right)\right] + \mathcal{O}(\epsilon^6). \tag{17}$$

These equations, on rescaling, become the two-dimensional version of the energy equation (see, for example, Landau and Lifschitz pg. 58 [14]).

188

4.2 The three-dimensional generalized von Kármán equations

In three dimensions, the equations may be decomposed as follows.

For a displacement (ξ, η, ζ), the in-plane strains are given by

$$e_{xx} = \xi_{,x} + \frac{1}{2}\zeta_{,x}^2, \quad e_{yy} = \eta_{,y} + \frac{1}{2}\zeta_{,y}^2, \quad e_{xy} = \frac{1}{2}\left(\xi_{,y} + \eta_{,x} + \zeta_{,x}\zeta_{,y}\right), \tag{18}$$

from which the in-plane stresses may be obtained

$$N_x = \frac{2d\mathcal{E}}{1 - \nu^2}(e_{xx} + \nu e_{yy}), \quad N_y = \frac{2d\mathcal{E}}{1 - \nu^2}(\nu e_{xx} + e_{yy}), \quad N_{xy} = \frac{2d\mathcal{E}}{1 + \nu}e_{xy}, \tag{19}$$

where $\mathcal{E} = \tilde{\mu}(3\tilde{\lambda} + 2\tilde{\mu})/(\tilde{\lambda} + \tilde{\mu})$ is Young's modulus, $\nu = \tilde{\lambda}/2(\tilde{\lambda} + \tilde{\mu})$ is the Poisson ratio and d is the half-thickness of the plate.

This gives the in-plane part of the generalized von Kármán equations as

$$N_{x,x} + N_{xy,y} = t_x, \quad N_{xy,x} + N_{y,y} = t_y \tag{20}$$

and the flexural part of the generalized von Kármán equations is described by

$$B\nabla_H^4\zeta = -t_z + (N_x\zeta_{,x} + N_{xy}\zeta_{,y})_{,x} + (N_{xy}\zeta_{,x} + N_y\zeta_{,y})_{,y} + dt_{x,x} + dt_{y,y}, \tag{21}$$

where $B = 2d^3\mathcal{E}/3(1 - \nu^2)$ is the flexural rigidity of the material, (t_x, t_y, t_z) is the traction on the base of the plate and $\nabla_H^4 = (\partial_x^2 + \partial_y^2)^2$.

4.3 Fluid equations

The fluid is assumed very viscous and so the Stokes' equations are used as the governing equations with

$$\mu\nabla^2\mathbf{u} = \boldsymbol{\nabla}p + \rho g(-\sin\theta, 0, \cos\theta), \quad \nabla \cdot \mathbf{u} = 0, \tag{22}$$

where $\mathbf{u} = (u, v, w)$ is the fluid velocity, p pressure, μ fluid viscosity, ρ fluid density, g gravity and θ the angle of the slope of the system. The x-axis is assumed to point downslope, y across slope and z perpendicular to the slope.

4.4 Interface conditions

At the interface between the plate and the fluid, we require continuity of velocity

$$\left.\frac{\partial\boldsymbol{\xi}}{\partial t}\right|_{\mathbf{X}} = \frac{\partial\boldsymbol{\xi}}{\partial t} + \mathbf{u} \cdot \nabla_{\mathbf{x}}\boldsymbol{\xi} = \mathbf{u}. \tag{23}$$

It should be noted that this is the only place where there is time dependence in the governing system of equations.

The tractions on the top of the plate are taken to be zero, and those on the bottom of the plate are

$$t_x = \hat{\mathbf{t}}_1 \cdot \boldsymbol{\sigma}_f \cdot \hat{\mathbf{n}}, \quad t_y = \hat{\mathbf{t}}_2 \cdot \boldsymbol{\sigma}_f \cdot \hat{\mathbf{n}}, \quad t_z = \hat{\mathbf{n}} \cdot \boldsymbol{\sigma}_f \cdot \hat{\mathbf{n}},$$

where $\boldsymbol{\sigma}_f$ is the fluid stress at the plate boundary, $\hat{\mathbf{n}}$ is the unit normal to the (base of the) plate and $\hat{\mathbf{t}}_1$, $\hat{\mathbf{t}}_2$ are the tangents to the plate aligned with x- and y-axis respectively. To as many terms as we need in our problems, these tractions become

$$t_x = \mu(u_{,z} + w_{,x}) - 2\mu(u_{,x} - w_{,z})\zeta_{,x} - \mu(u_{,y} + v_{,x})\zeta_{,y} \tag{24}$$

$$t_y = \mu(v_{,z} + w_{,y}) - 2\mu(v_{,y} - w_{,z})\zeta_{,y} - \mu(u_{,y} + v_{,x})\zeta_{,x} \tag{25}$$

$$t_z = -p + 2\mu w_{,z} - 2\mu(u_{,z} + w_{,x})\zeta_{,x} - 2\mu(v_{,z} + w_{,y})\zeta_{,y}. \tag{26}$$

4.5   Boundary conditions

The boundary conditions on the plate edges are given by fixed displacement, usually

$$\xi = \eta = \zeta = 0 \tag{27}$$

and a further condition on ζ, since the flexural equation (21) is fourth order. In our problems, the edges of the plate are at $y = $ const. and possibilities for the further boundary condition on ζ include $\zeta_{,y} = 0$, $\quad \zeta_{,yy} = 0$, $\quad \zeta_{,yyy} = 0$ for clamped, freely-supported or hinged respectively. For all the problems we study, we use a clamped boundary condition at the edges:

$$\zeta_{,y} = 0. \tag{28}$$

The fluid has zero velocity on rigid surfaces.

5   The problems

In this section, we consider three problems of fluid–plate interaction. The first problem, in §5.1, is the buckling of a compressed beam in contact with a two-dimensional very viscous fluid below it. This is a modification of the classical, purely elastic problem of beam buckling. It was first studied by Huang and Suo [19] using the lubrication equation to model the fluid. The motivation for considering this problem is to understand how the fluid modifies buckling.

The second problem, in §5.2, looks at flow in a channel down a slope. In this case there is no pre-compression on the system and the aim is to understand under what conditions the fluid induced shear on the plate can cause buckling.

Finally, in §5.3, we bring aspects from both of the previous problems together to try to begin to understand the wrinkles observed in our experiments of §3.

We use linear stability analysis to analyze our problems. This allows us to find when and where wrinkling can occur and is a relatively simple method. Linear stability analysis is not particularly relevant to pure elasticity cases because elastic waves are fast, and so the system quickly passes the linear growth regime. However, for a viscous fluid controlling the growth rate of any buckling instabilities in our problems, a linear stability analysis is more useful.

Our notation throughout is subscript 0 for base states and no subscripts for the perturbation flow. Derivatives are denoted as in §4 by subscript "$,\cdot$" for consistency.

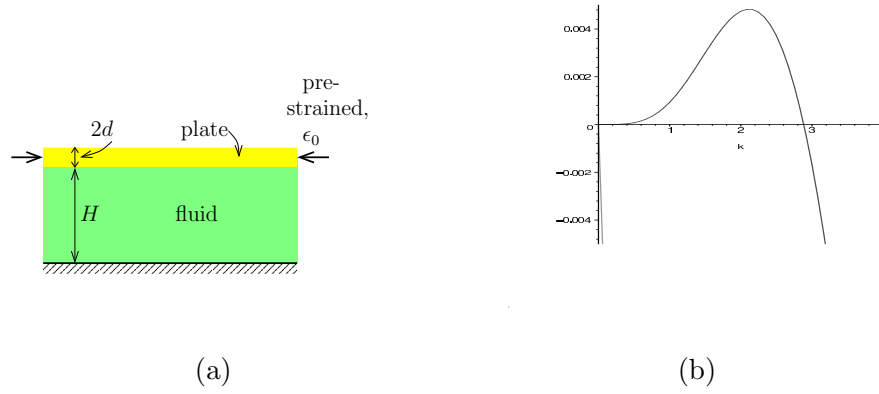<center>(a)   (b)</center>

Figure 5: (a) The configuration for the buckling of a beam above a very viscous fluid. (b) Growth rate, $\Im(\omega)$, versus wavenumber k. Note that one mode is very close to the negative $\Im(\omega)$-axis.

5.1 Two-dimensional simple buckling

In this subsection, we examine the buckling of a pre-compressed beam in contact with a two-dimensional very viscous fluid of depth H, as shown in figure 5(a). This problem was first investigated by Huang and Suo [19] in the context of the manufacture of semi-conductors. Our problem formalism is very similar to theirs, however we use the Stokes' equations for the fluid whereas they used the lubrication equation. Our results are essentially identical to theirs. In addition, Huang and Suo also performed a numerical simulation of the system. For this problem, gravity is ignored and the fluid is passive.

5.1.1 Base state

In the base state, everything is assumed to be zero, except for the normal strain e_{xx} which is non-zero. We refer to this as pre-strain, $e_{xx} = \epsilon_0$. Hence the system has a given pre-stress: compressive if $\epsilon_0 < 0$ and tensile if $\epsilon_0 > 0$.

5.1.2 Linearized perturbation

We now add a perturbation and linearize the governing system of equations (18)–(28) about the base state. In addition, we non-dimensionalize the equations using $L = H$ for lengths, $U = 2d\mathcal{E}/(1 - \nu^2)\mu$ for velocities, L/U for times and $\mu U/L$ for pressures. Note that the time scale of the problem depends on the fluid. We set $\delta_b = d/H$.

The governing equations then reduce to

$$\xi_{,xx} = u_{,z} + w_{,x}, \quad \frac{1}{3}\delta_b^2 \zeta_{,xxxx} = p - 2w_{,z} + \epsilon_0 \zeta_{,xx},$$

$$\nabla^2 \mathbf{u} = \boldsymbol{\nabla} p, \quad \nabla \cdot \mathbf{u} = 0,$$

$$\xi_{,t} = u, \quad \zeta_{,t} = w \quad \text{on } z = 1,$$

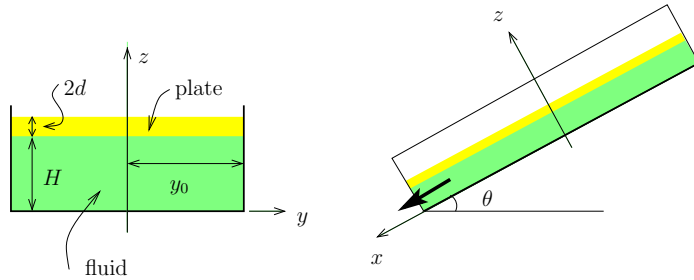$$\mathbf{u} = 0 \quad \text{on } z = 0,$$

<center>191</center>

Figure 6: Configuration for channel flow. The fluid is confined by rigid walls at $y = \pm y_0$, and $z = 0$ and an elastic plate at $z = H$. The fluid flows due to gravity alone.

for the plate equations, fluid equations, interface conditions and boundary conditions respectively.

If we now look for solutions proportional to $e^{ikx - i\omega t}$, these equations reduce to

$$
\det \begin{pmatrix} \sinh k + k \cosh k + 2\Omega(\cosh k + k \sinh k) & -k^2 \sinh k - 2\Omega k^2 \cosh k \\[2ex] \left(\frac{1}{3}\delta_b^2 k^2 + \epsilon_0\right)\sinh k & \left(\frac{1}{3}\delta_b^2 k^2 + \epsilon_0\right)(\sinh k - k \cosh k) \\ -\delta_b(\sinh k + k \cosh k) + 2\Omega \cosh k & +\delta_b k^2 \sinh k + 2\Omega(\cosh k - k \sinh k) \end{pmatrix} = 0,
$$

where $\Omega = -i\omega/k$, to give the dispersion relation. Figure 5(b) shows the two solution branches for $\Im(\omega)$ against k, for the specific choice of parameters $\epsilon_0 = -0.0156$, $\delta_b = 0.075$. As can be seen, one root is negative for all k and hence the perturbation is stable, whereas the other is positive for small k, and hence the perturbation is unstable. The short-wave cut-off occurs at $\delta_b^2 k^2/3 + \epsilon_0 = 0$ and is due to flexural rigidity preventing shorter waves.

The main contribution of the fluid is setting the time-scale: its presence reduces the rate at which the instability grows, because it only slowly flows out of the way of the buckling plate (Huang and Suo).

5.2 Channel flow

In this subsection we examine the flow of a very viscous fluid in a channel of half-width y_0, down a slope of angle θ. The side walls and base of the channel are rigid and the top, at $z = H$, is an elastic plate, clamped at its edges across the slope. The fluid flow is due only to gravity: there is no imposed pressure gradient. It is assumed that the volume flux of fluid is exactly sufficient to keep the elastic plate flat in its base state. This configuration is shown in figure 6.

This is closely related to a much studied classical problem in elasticity: a thin plate in shear (see, for example, Wong and Pellegrino [20]). In this case the configuration is a plate whose long edges are attached to rigid rods held a fixed distance apart, so that the plate is just taut. One of the rods is then translated parallel to its length. Wrinkles are observed between the rods, at 45°, regardless of the amplitude of the displacement of the rod. This is a result of the Poisson effect: although the plate is under tension in the direction of the major principal stress, it is in compression in the direction of minor principal stress with the

result that buckling occurs. This problem has been approached in a variety of ways. The original method was using tension field theory, see for example Mansfield [21], which was able to predict the 45° angle of the wrinkle.[3] More recently, Wong and Pellegrino [22] found simple analytic predictions using an assumed form for the out-of-plane displacement and force or energy minimization arguments. In addition, experiments and many finite element computations have been performed (see, for example Wong and Pellegrino [20]).

The aim of this section is to show that, in our problem, the traction of the fluid on the bottom of the elastic plate, results in a similar buckling phenomenon.

5.2.1   Base flow

For the base state, we assume that the fluid flow is purely down-slope with $v_0 = w_0 = 0$. We assume that the plate is not displaced in the cross-slope direction, so $\eta_0 = 0$, and that it suffers no out-of-plane displacement, hence $\zeta_0 = H$. The system is assumed independent of the downslope coordinate, x, and time, t. Hence we take

$$u = u_0(y, z), \qquad \xi = \xi_0(y), \qquad p = p_0(z).$$

The governing equations for the fluid (22) in the base state become

$$\mu(u_{0,yy} + u_{0,zz}) = -\rho g \sin\theta, \quad 0 = p_{0,z} + \rho g \cos\theta, \tag{29}$$

with boundary conditions

$$u_0 = 0 \qquad \text{on } z = 0, H; \ y = \pm y_0. \tag{30}$$

This system is identical to that for flow in a rigid rectangular duct: the fact that the upper surface is elastic is immaterial (except for the pressure being known at the upper surface, see below).

The in-plane deformation equations for the plate (20) reduce to

$$\frac{d\mathcal{E}}{1+\nu} \xi_{0,yy} = \mu u_{0,z}, \tag{31}$$

with boundary condition $\xi_0 = 0$ at $y = \pm y_0$. The flexure equation (21) reduces to $p_0 = 0$ on $z = H$, completing the pressure equation (29b).

Using Fourier series for u_0, this system can be solved giving

$$p_0 = \rho g \cos\theta\,(H - z), \tag{32}$$

$$u_0 = \rho g \sin\theta\, H^2/\mu\, \mathcal{U}(Y, Z; \alpha), \tag{33}$$

$$\xi_0 = y_0^2 \rho g \sin\theta\, H(1+\nu)/d\mathcal{E}\, \Xi(Y; \alpha), \tag{34}$$

where $Y = y/y_0$, $Z = z/H$, $\alpha = H/y_0$ and

$$\mathcal{U}(Y, Z; \alpha) = \frac{16}{\pi^4} \sum_{n,m=0}^{\infty} \frac{(-1)^m \sin[(2n+1)\pi Z]\cos[(2m+1)\pi Y/2]}{(2n+1)(2m+1)[(2n+1)^2 + \alpha^2(2m+1)^2/4]},$$

$$\Xi(Y; \alpha) = \frac{64}{\pi^5} \sum_{n,m=0}^{\infty} \frac{(-1)^m \cos[(2m+1)\pi Y/2]}{(2m+1)^3[(2n+1)^2 + \alpha^2(2m+1)^2/4]}.$$

---

[3]Unfortunately, we cannot use tension field theory, as it relies on the existence of an Airy stress function: one no longer exists for the generalized von Kármán equations.
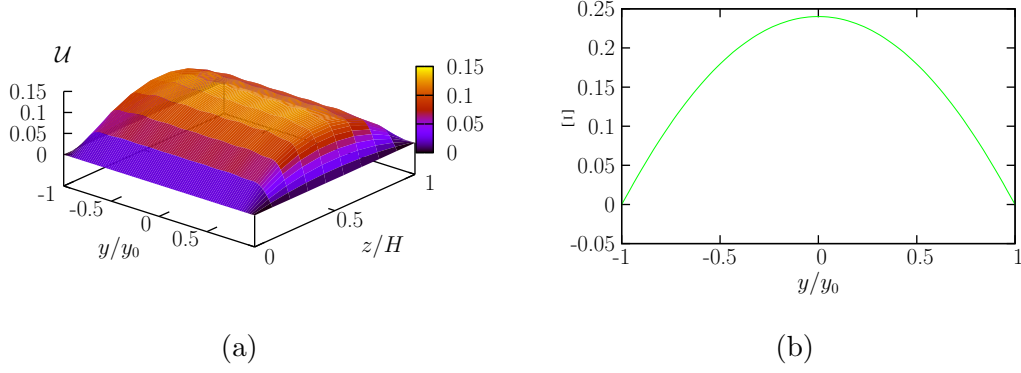
Figure 7: (a) Velocity profile, $\mathcal{U}$, against $Y = y/y_0$ and $Z = z/H$ and (b) downstream displacement of the plate, Ξ, against Y for $\alpha = 0.25$.

Plots of solutions for $\mathcal{U}$ and Ξ are shown in figure 7 for $\alpha = 0.25$. As can be clearly seen, the fluid pulls the plate downstream.

To be compatible with the scalings assumed to obtain the generalized von Kármán plate equations, we must be in a regime in which the displacement is small. For this we use the strict scaling $\xi \sim d^2/L$ and hence we require

$$\mathfrak{E}_c = \frac{\mathcal{E}d^3}{\rho g \sin\theta\, H y_0^3} \sim 1. \tag{35}$$

5.2.2   Linearized perturbation

We now add a small perturbation to the base state and consider the linearized equations governing the system.

The linearized perturbation equations for the plate then become

$$\frac{2d\mathcal{E}}{1-\nu^2}(\xi_{,xx} + \nu\eta_{,xy}) + \frac{d\mathcal{E}}{1+\nu}(\xi_{,yy} + \eta_{,xy}) = \mu u_{0,zz}\zeta - \mu u_{0,y}\zeta_{,y} + \mu(u_{,z} + w_{,x}), \tag{36}$$

$$\frac{d\mathcal{E}}{1+\nu}(\xi_{,xy} + \eta_{,yy}) + \frac{2d\mathcal{E}}{1-\nu^2}(\nu\xi_{,xy} + \eta_{,yy}) = -\mu u_{0,y}\zeta_{,x} + \mu(v_{,z} + w_{,y}), \tag{37}$$

for the in-plane deformation equations (20) and

$$B\nabla_H^4\zeta = p_{0,z}\zeta + 2\mu u_{0,z}\zeta_{,x} + p - 2\mu w_{,z} + 2\frac{d\mathcal{E}}{1+\nu}\xi_{0,y}\zeta_{,xy} + \frac{d\mathcal{E}}{1+\nu}\xi_{0,yy}\zeta_{,x}$$

$$+ d[-\mu u_{0,y}\zeta_{,xy} + \mu u_{0,zz}\zeta_{,x} + \mu(u_{,xz} + w_{,xx}) - \mu u_{0,yy}\zeta_{,x} - \mu u_{0,y}\zeta_{,xy} + \mu(v_{,yz} + w_{,yy})], \tag{38}$$

for the flexural equation (21). The boundary conditions for the plate, from (27) and (28), are

$$\xi = \eta = \zeta = \zeta_{,y} = 0 \qquad \text{at } y = \pm y_0. \tag{39}$$

The linearized perturbation equations for the fluid, from (22), become

$$\mu\nabla^2 u = p_{,x}, \quad \mu\nabla^2 v = p_{,y}, \quad \mu\nabla^2 w = p_{,z}, \quad u_{,x} + v_{,y} + w_{,z} = 0, \tag{40}$$

194

with boundary conditions

$$u = v = w = 0 \qquad \text{on } z = 0; \ y = \pm y_0. \tag{41}$$

The condition of continuity of velocity at the interface (23) becomes

$$\xi_{,t} + v\xi_{0,y} = u + u_{0,z}\zeta, \quad \eta_{,t} = v, \quad \zeta_{,t} = w. \tag{42}$$

These equations appear fairly complex, however we can make some significant simplifications by neglecting terms which are order d/L smaller than the leading order terms (in fact, we must do this as it not consistent to keep them). Here L is the horizontal length scale for the perturbation, assumed to satisfy $L \ll y_0$. We scale according to (8) in the derivation and bear in mind the different length-scale for the base state. We also scale vertical derivatives with L as we would like vertical and horizontal length scales to be similar. We then have from $t_z \sim \mathcal{E}d^4/L^4$ in (8), as $\mathcal{E} \sim \mu$, that $p \sim \mathcal{E}d^4/L^4$, from which $u \sim \mathcal{E}/\mu \, d^4/L^3$ using (40). Substituting these into (36)–(38) and (42) we obtain the reduced system

$$\frac{2d\mathcal{E}}{1 - \nu^2}(\xi_{,xx} + \nu\eta_{,xy}) + \frac{d\mathcal{E}}{1 + \nu}(\xi_{,yy} + \eta_{,xy}) = \mu u_{0,zz}\zeta, \tag{43}$$

$$\frac{d\mathcal{E}}{1 + \nu}(\xi_{,xy} + \eta_{,yy}) + \frac{2d\mathcal{E}}{1 - \nu^2}(\nu\xi_{,xy} + \eta_{,yy}) = 0 \tag{44}$$

for the in-plane equations,

$$B\nabla_H^4\zeta = p_{0,z}\zeta + 2\mu u_{0,z}\zeta_{,x} + p - 2\mu w_{,z} + 2\frac{d\mathcal{E}}{1 + \nu}\xi_{0,y}\zeta_{,xy} + \frac{d\mathcal{E}}{1 + \nu}\xi_{0,yy}\zeta_{,x} \tag{45}$$

for the flexural equation and

$$0 = u + u_{0,z}\zeta, \quad 0 = v, \quad \zeta_{,t} = w \quad \text{on } z = H \tag{46}$$

for the interface conditions. The fluid remains as in (40) and boundary conditions remain (39) and (41).

To gain an understanding of the instability, we look for small wavelength solutions and we assume the background variation is slow in comparison. This allows us to Fourier decompose the perturbation in both the x- and the y-direction. Ultimately, this could be made rigorous using WKB.

Therefore we assume the perturbation is proportional to $e^{ikx+ily-i\omega t}$ and we ignore cross-stream boundary conditions.

Solving (40) subject to $u = v = w = 0$ on $z = 0$, and (46) on $z = H$, we obtain

$$p - 2\mu w_{,z} = 2\mu Ki\omega\frac{\cosh KH \sinh KH + KH}{\sinh^2 KH - K^2H^2}\zeta + u_{0,z}\frac{2\mu ikK^2H^2}{\sinh^2 KH - K^2H^2}\zeta,$$

where $K^2 = k^2 + l^2$. Hence (45) becomes

$$BK^4\zeta = -\rho g \sin\theta \, \zeta + 2\mu Ki\omega\frac{\cosh KH \sinh KH + KH}{\sinh^2 KH - K^2H^2}\zeta + 2\mu iku_{0,z}\frac{\sinh^2 KH}{\sinh^2 KH - K^2H^2}\zeta$$
$$- \frac{2d\mathcal{E}}{1 + \nu}\xi_{0,y}kl\zeta + \frac{d\mathcal{E}}{1 + \nu}ik\xi_{0,yy}\zeta.$$
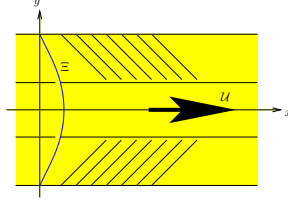
Figure 8: Cartoon (plan view) of the observed instability for the channel flow. The angled lines represent wrinkle crests. The interior area is wrinkle free.

This relation only depends on ζ and hence the dispersion relation becomes

$$-2\mu K\frac{\cosh KH \sinh KH + KH}{\sinh^2 KH - K^2 H^2}i\omega = -BK^4 - \rho g\cos\theta$$

$$-2y_0\rho g\sin\theta\, H\,\Xi'(Y;\alpha)kl + ik\frac{3\sinh^2 KH - K^2 H^2}{\sinh^2 KH - K^2 H^2}\rho g\sin\theta\, H\Xi''(Y;\alpha), \quad (47)$$

using (31) and (34).

From the dispersion relation some of the properties of the instability may be deduced. We consider $\Im(\omega)$, and note that the coefficient of $i\omega$ is positive for all (k,l). The first two terms on the right hand side of (47) result from the flexural term and hydrostatic pressure. Both are always negative and hence stabilizing. The third term results from the base displacement of the plate due to fluid traction on the base and can be destabilizing. A necessary condition for instability is $kl\Xi'(Y;\alpha) < 0$. Hence any observed crests will be oriented downstream, as shown in figure 8. In the interior $\Xi' = 0$ and close by it is too small to overcome the stabilizing flexural and hydrostatic pressure terms. Hence, in an interior region, no wrinkles are observed. The final term of (47) is imaginary and hence not directly important to the stability.

Finally, if we look at a fastest growing mode, then the observed modes have $k = \pm l$. This suggests that even for a small displacement due to fluid traction, the wrinkles will have a significant angle.

There is much that needs to be done to complete this analysis, and check for its consistency with scalings.

5.3 Rivulet flow

In this subsection we study the flow of a very viscous fluid, contained between a rigid base and an elastic plate clamped to the base along lines $y = \pm y_0$. This configuration is shown in figure 9. It is close to the physical situation we wish to model and is equivalent to our experiments of §3. In this scenario, there is a combination of pre-strain, as in §5.1, and fluid traction on the base of the plate, as in §5.2, to produce buckling; bringing together the features of the previous two problems.

First consider the elastic plate in the absence of the fluid. It has approximate unstressed length $2(1 - \epsilon_0)y_0$, or equivalently a pre-strain $e_{yy} = \epsilon_0$, where $|\epsilon_0| \ll 1$. If $\epsilon_0 > 0$, then the plate is in tension and is flat against the base. If $\epsilon_0 < 0$, then the plate is in compression and will buckle. Hence this pre-compression may be conceptualized as slack.
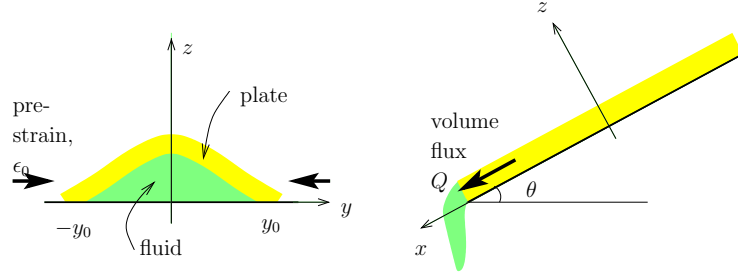
Figure 9: Configuration for the rivulet problem. An elastic plate is clamped to a rigid base along lines $y = \pm y_0$ and fluid is introduced into the gap between.

If fluid is now introduced between the rigid base and the taut plate for $\epsilon_0 > 0$, then it forces the plate out of the plane of the base, and increases the tension on it, and no instability is found. For $\epsilon_0 < 0$, the situation is more complex. If sufficient fluid is introduced, then the increased out-of-plane displacement is sufficient for the plate to be taut. However, if a small volume of fluid is introduced, some compressive sress may remain and the plate still buckles. In any case, the plate is forced out of the plane of the base by the fluid, stretched across stream to accommodate the fluid and pulled downstream by the fluid.

5.3.1   Base flow

We use the governing system of equations (18)–(28), non-dimensionalizing the variables by y_0 for lengths, $\rho g \cos \theta \, y_0$ for pressures and elastic stresses and $\rho g \sin \theta \, y_0^2 / \mu$ for velocities. We also set $\mathfrak{E}_r = 2d\mathcal{E}/(1 - \nu^2)\rho g \cos \theta \, y_0^2$, representing a ratio of elastic stress to fluid pressure, and put $\delta_r = d/y_0$.

The base state is assumed independent of down-stream coordinate, x, and $v_0 = w_0 = 0$ is assumed.

The in-plane plate equations (20) reduce to

$$\frac{1}{2}(1 - \nu)\mathfrak{E}_r \xi_{0,yy} = u_{0,z} - u_{0,y}\zeta_{0,y}, \quad \mathfrak{E}_r \left(\epsilon_0 + \eta_{0,y} + \frac{1}{2}\zeta_{0,y}^2 \right) = \text{const.} = \mathfrak{E}_r N_0, \qquad (48)$$

where ϵ_0 is the imposed pre-strain and the dependent variable N_0 may be interpreted as the remaining pre-stress. Note that, unlike in Euler's elastica problem, the stress is a dependent variable whereas the displacement is a parameter. The flexure equation (21) becomes

$$\frac{1}{3}\delta_r^2 \mathfrak{E}_r \zeta_{0,yyyy} = p_0 + \mathfrak{E}_r N_0 \zeta_{0,yy}, \qquad (49)$$

and the boundary conditions on the plate are

$$\xi_0 = \eta_0 = \zeta_0 = \zeta_{0,y} = 0 \qquad \text{at } y = \pm 1. \qquad (50)$$

The fluid equations (22) become

$$u_{0,yy} + u_{0,zz} = -1 \qquad (51)$$

197

for the downstream flow and

$$p_0 = \tilde{p}_0 - z \qquad (52)$$

for hydrostatic pressure, where $\tilde{p}_0$ is a constant of integration. The boundary conditions on the plate are

$$u_0 = 0 \qquad \text{on } z = 0, \ \zeta_0(y). \qquad (53)$$

The final condition on the system is constant imposed volume flux[4]

$$\frac{1}{6}Q = \int_{-1}^{1} \int_{0}^{\zeta_0(y)} u_0(y', z) \, \mathrm{d}z \, \mathrm{d}y', \qquad (54)$$

where the flux has been non-dimensionalized by $\rho g \sin\theta \, y_0^4/6\mu$.

Equation (51) subject to the boundary condition (53) is a complex system to solve, more so as the solution for ζ_0 depends on condition (54). However, in view of the scalings (8) used to obtain the von Kármán equations, the vertical length-scale for the fluid must be much less than the horizontal. Hence a lubrication-like approximation may be made and (51) replaced by

$$u_{0,zz} = -1,$$

with solution satisfying (53) given by

$$u = z[\zeta_0(y) - z].$$

Condition (54) thus becomes

$$Q = \int_{-1}^{1} \zeta_0^3(y) \, \mathrm{d}y. \qquad (55)$$

We now look at solutions for the governing system of equations (48)–(53) and (55). First we consider the solution for ζ_0. Substituting (52) into (49) and solving for ζ_0 subject to the boundary conditions (50c,d) we obtain

$$\zeta_0(y) = \tilde{p}_0 \left(\frac{-m_2 \sinh m_2 \cosh m_1 y + m_1 \sinh m_1 \cosh m_2 y}{m_2 \sinh m_2 \cosh m_1 - m_1 \sinh m_1 \cosh m_2} + 1 \right), \qquad (56)$$

where

$$m_{1,2} = \sqrt{\frac{\mathfrak{E}_r N_0 \pm \sqrt{\mathfrak{E}_r^2 N_0^2 - \frac{4}{3}\delta_r^2 \mathfrak{E}_r}}{\frac{2}{3}\delta_r^2 \mathfrak{E}_r}}.$$

The behaviour of this solution depends on the sign and magnitude of $\mathfrak{E}_r N_0$. For $\mathfrak{E}_r N_0 < -\sqrt{4\delta_r^2 \mathfrak{E}_r/3}$, m_i are purely imaginary, and the hyperbolic cosine terms in (56) become cosines, giving an oscillating solution for ζ_0. For $\mathfrak{E}_r N_0 > \sqrt{4\delta_r^2 \mathfrak{E}_r/3}$, m_i are real and the solution consists of hyperbolic cosine terms, and lacks oscillations. For $|\mathfrak{E}_r N_0| < \sqrt{4\delta_r^2 \mathfrak{E}_r/3}$,

---

[4]If the system were on a flat base, then this final condition would be a fixed volume constraint

$$V = \int_{-1}^{1} \zeta_0(y) \, \mathrm{d}y.$$

The analysis for this case is similar to that presented for the fixed flux. It is also related to work by Riera and Mahadevan [23] on the drying of sessile drops.

the solution for ζ_0, (56), becomes a sum of products of hyperbolic cosines and cosines. Note that, regardless of the value of $\mathfrak{E}_r N_0$, the form in (56) is real.[5]

N_0 and $\tilde{p}_0$ are still unknowns that must be specified. If we assume N_0 is known, then $\tilde{p}_0$ may be found from (55) to give

$$\tilde{p}_0 = \left(Q \Big/ \int_{-1}^{1} (\zeta_0/\tilde{p}_0)^3 \, \mathrm{d}y \right)^{\frac{1}{3}}. \tag{57}$$

This eliminates the singularity in the denominator of ζ_0 in (56) at $m_1 \tanh m_1 = m_2 \tanh m_2$, however it introduces a new one where $\int_{-1}^{1}(\zeta_0/\tilde{p}_0)^3 \, \mathrm{d}y = 0$.

Finally, N_0 may be found by solving (48b) for η_0. Subject to boundary condition (50b), the solution is

$$\eta_0 = \frac{y+1}{4} \int_{-1}^{1} \zeta_{0,y}^2 \, \mathrm{d}y - \frac{1}{2} \int_{-1}^{y} \zeta_{0,y'}^2 \, \mathrm{d}y',$$

from which we obtain

$$N_0 = \epsilon_0 + \frac{1}{4} \int_{-1}^{1} \zeta_{0,y}^2 \, \mathrm{d}y. \tag{58}$$

Hence we may treat the problem as an inverse one: we fix the dependent variable N_0, which provides the full solution for ζ_0, and calculate the imposed parameter ϵ_0 as a function of N_0 using (58).

We may write this relation

$$\mathfrak{E}_r \epsilon_0 = \mathfrak{E}_r N_0 - \frac{(\mathfrak{E}_r^{3/2} Q)^{2/3} \int_{-1}^{1} (\zeta_{0,y}/\tilde{p}_0)^2 \, \mathrm{d}y}{\left(\int_{-1}^{1} (\zeta_{0,y}/\tilde{p}_0)^3 \, \mathrm{d}y \right)^{2/3}}.$$

Hence note that by scaling the parameters, ϵ_0, Q and δ_r, and the dependent variables, N_0, $\tilde{p}_0$ and ζ_0, appropriately, we eliminate explicit dependence on the parameter $\mathfrak{E}_r$.

Figure 10(a) shows a contour plot of the scaled pre-strain, $\mathfrak{E}_r \epsilon_0$, against $\mathfrak{E}_r N_0$ and the scaled volume flux, $\mathfrak{E}_r^{3/2} Q$. For a given $\mathfrak{E}_r \epsilon_0 < 0$, and a given value of $\mathfrak{E}_r^{3/2} Q$, there are multiple possible values of $\mathfrak{E}_r N_0$. The system has non-unique solutions: a feature of buckling.

Figure 10(b) shows the full set of solutions for the choice of parameters $\mathfrak{E}_r^{3/2} Q = 1$ and $\mathfrak{E}_r \epsilon_0 = -3$. Solutions which go below the y-axis are physically not allowed, however there still remain several valid solutions. The green curve (plotted with $\zeta_0(-1) = 4.5$) is the solution we choose for the system, based on an energy minimization argument, as discussed below.

There are some other notable features of the plot. The solid, black vertical lines satisfy

$$\int_{-1}^{1} (\zeta_0/\tilde{p}_0)^3 \, \mathrm{d}y = 0, \tag{59}$$

---

[5]There are a couple of other points to note. Firstly, the form of the solution (56) is single-valued although this is not necessarily physically correct. Secondly, if δ_r becomes too small, then the flexural term should be neglected from the plate equations (21). Note also, that if there are too many wiggles, then the assumption that the horizontal length-scale for the plate is much larger than the vertical also fails.
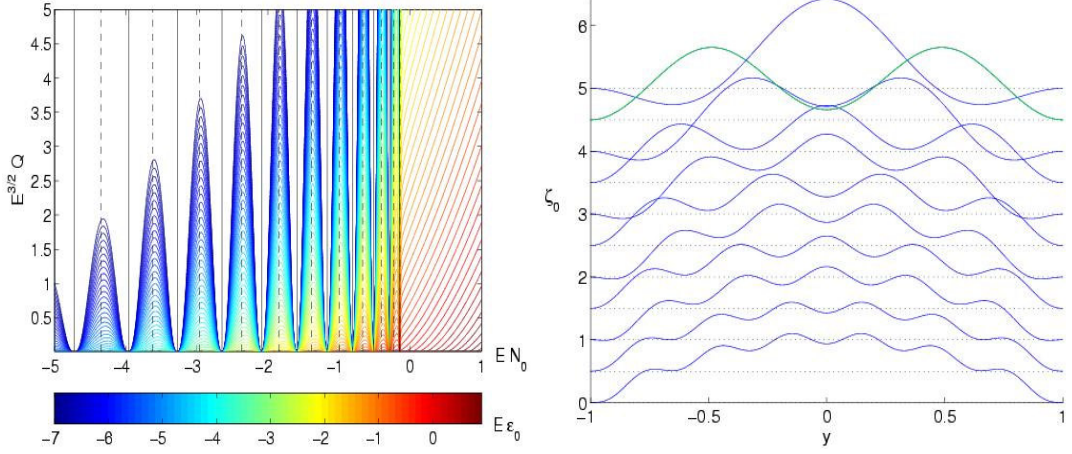
Figure 10: (a) Contours of the imposed parameter $\mathfrak{E}_r\epsilon_0$ against the dependent variable $\mathfrak{E}_r N_0$ and parameter $\mathfrak{E}_r^{3/2}Q$. For a given value of $\mathfrak{E}_r\epsilon_0$ there corresponds a contour. Then, for a given value of $\mathfrak{E}_r^{3/2}Q$ there are multiple possible values of $\mathfrak{E}_r N_0$, and hence multiple possible solutions for ζ_0. The solid and dashed vertical lines satisfy (59) and (60) respectively. (b) Solutions of ζ_0 for the choice of parameters $\mathfrak{E}_r^{3/2}Q = 1$ and $\mathfrak{E}_r\epsilon_0 = -3$. The lowest solution corresponds to the smallest solution for $\mathfrak{E}_r N_0$, and higher up solutions correspond to larger values of $\mathfrak{E}_r N_0$. The green curve (plotted with $\zeta_0(-1) = 4.5$) is the curve chosen on the basis of minimum energy.
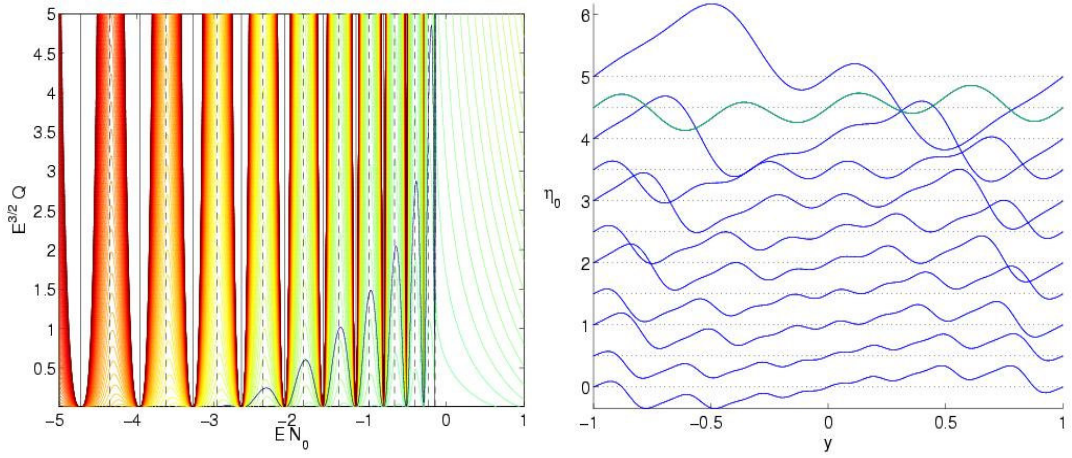

Figure 11: (a) Contours of plot of energy against $\mathfrak{E}_r N_0$ and $\mathfrak{E}_r^{3/2}Q$ together with the contour $\mathfrak{E}_r\epsilon_0 = -3$. The solid and dashed lines again satisfy (59) and (60) respectively. (b) Solutions of η_0 for the choice of parameters $\mathfrak{E}_r^{3/2}Q = 1$ and $\mathfrak{E}_r\epsilon_0 = -3$. The lowest solution corresponds to the smallest solution for $\mathfrak{E}_r N_0$, and higher up solutions correspond to larger values of $\mathfrak{E}_r N_0$. The green curve is the curve chosen on the basis of minimum energy.

200

or equivalently are where $\tilde{p}_0$ is infinite from (57). Across these lines, the solution ζ_0 is reflected in the y-axis. The dashed black lines satisfy

$$\frac{1}{m_1} \tanh m_1 = \frac{1}{m_2} \tanh m_2 \tag{60}$$

and occur when $\zeta_{0,yy}/\tilde{p}_0 = 0$ at $y = \pm 1$. In regions with solid lines to the left and dashed lines to the right, $\zeta_{0,yy} < 0$ at $y = \pm 1$ and in regions with dashed lines to the left and solid lines to the right, $\zeta_{0,yy} > 0$ at $y = \pm 1$. Hence only the latter are physically acceptable. At dashed lines, as $\mathfrak{E}N_0$ increases, two extra down-wiggles are created. At the next solid line, the shape is reflected so the down-wiggles become up-wiggles. Hence, beginning with one up-wiggle and zero down-wiggles in the right-most finger of figure 10(a), there is one more up-wiggle in each finger to the left.

The choice of solution for a given set of parameters must still be made. We select the minimum energy solution.

The total energy of the system is divided into two parts: the internal (stretching and bending) energy of the elastic plate and the potential energy of the fluid. The two components of the plate energy per unit area are given by (16)

$$\psi_{\text{bending}} = \frac{1}{3}\delta_r^2 \mathfrak{E}_r \zeta_{0,yy}^2, \quad \psi_{\text{stretching}} = \mathfrak{E}_r \left[\frac{1}{2}(1-\nu)\xi_{0,y}^2 + N_0^2 \right]$$

respectively, where the energies have been non-dimensionalized by $\rho g \cos\theta\, y_0^2/2$. The potential energy of the fluid per unit area is

$$\psi_{\text{potential}} = \zeta_0^2.$$

For zero Reynolds' number flows, the kinetic energy is negligible. Hence the total energy per unit length becomes

$$\mathfrak{E}_r \Psi_{\text{total}} = \frac{1}{3}\delta_r^2 \mathfrak{E}_r \int_{-1}^{1} \mathfrak{E}_r \zeta_{0,yy}^2 \,dy + 2(\mathfrak{E}_r N_0)^2 + \frac{1}{2}(1-\nu)\int_{-1}^{1} \mathfrak{E}_r^2 \xi_{0,y}^2 \,dy + \int_{-1}^{1} \mathfrak{E}_r \zeta_0^2 \,dy.$$

Note that this expression again has no explicit dependence on $\mathfrak{E}_r$.

Figure 11(a), shows a plot of energy contours against $\mathfrak{E}_r N_0$ and $\mathfrak{E}_r^{3/2}Q$, together with the contour $\mathfrak{E}_r \epsilon_0 = -3$. In this case, the solution with minimum energy is seen to correspond to the one with least wiggles. This is because there is little compressive stress remaining in this case. This analysis is perhaps not quite correct though: the cross-stream displacement η_0 is shown in figure 11(b) and it is seen to increase as the number of wiggles decreases. It might have been expected that more wiggles would be preferable so that the plate fits more easily over a given volume of fluid.

5.3.2 Linearized perturbation

We now consider the stability of this base state to small perturbations. The linearized perturbation equations for the plate are

$$\frac{2d\mathcal{E}}{1-\nu^2}(\xi_{,xx} + \nu\eta_{,xy} + \nu\zeta_{0,y}\zeta_{,xy}) + \frac{d\mathcal{E}}{1+\nu}(\xi_{,yy} + \eta_{,xy} + \zeta_{0,yy}\zeta_{,x} + \zeta_{0,y}\zeta_{,xy}) = \mu u_{0,zz}\zeta,$$

$$\frac{d\mathcal{E}}{1+\nu}(\xi_{,xy} + \eta_{,yy} + \zeta_{0,y}\zeta_{,xx}) + \frac{2d\mathcal{E}}{1-\nu^2}(\nu\xi_{,xy} + \eta_{,yy} + \zeta_{0,yy}\zeta_{,y} + \zeta_{0,y}\zeta_{,yy}) = 0$$

201

for the in-plane plate equations (20) and

$$B\nabla_H^4 \zeta = p_{0,z}\zeta + 2\mu u_{0,z}\zeta_{,x} + p - 2\mu w_{,z} + \rho g\cos\theta\, y_0^2 N_0(\nu\zeta_{,xx} + \zeta_{,yy}) + 2\frac{d\mathcal{E}}{1+\nu}\xi_{0,y}\zeta_{,xy}$$

$$+ \frac{2d\mathcal{E}}{1-\nu^2}\zeta_{0,yy}(\nu\xi_{,x} + \eta_{,y} + \zeta_{0,y}\zeta_{,y}) + \frac{d\mathcal{E}}{1+\nu}\xi_{0,yy}\zeta_{,x}$$

for the flexural equation (21), with boundary conditions (27) and (28)

$$\xi = \eta = \zeta = \zeta_{,y} = 0 \qquad \text{at } y = \pm y_0.$$

The linearized perturbation equations for the fluid (22) are

$$\mu\nabla^2 u = p_{,x}, \quad \mu\nabla^2 v = p_{,y}, \quad \mu\nabla^2 w = p_{,z}, \quad u_{,x} + v_{,y} + w_{,z} = 0,$$

with boundary conditions

$$u = v = w = 0 \qquad \text{on } z = 0; \ y = \pm y_0.$$

Finally, the linearized interface conditions (23) are

$$0 = u + u_{0,z}\zeta, \quad 0 = v, \quad \zeta_{,t} = w \quad \text{on } z = H.$$

We set $L_p' < \zeta_0(0)$ and $L_p < y_0$ to be the out-of-plane and in-plane length-scales of the perturbation repectively. Then we have neglected terms that are $\mathcal{O}(L_p'/L_p)$, smaller than the leading order terms in each of these equations, as in §5.2.2.

Assuming perturbations are small wavelength and background variation of the base state is slow, we substitute solutions proportional to $e^{ikx+ily-i\omega t}$ into the above equations and derive a dispersion relation with real part

$$2\mu K\frac{\cosh K\zeta_0\sinh K\zeta_0 + K\zeta_0}{\sinh^2 K\zeta_0 - K^2\zeta_0^2}\, \Im(\omega) = -BK^4 - \rho g\cos\theta$$

$$- \rho g\cos\theta\, y_0^2 N_0(\nu k^2 + l^2) - 2\frac{d\mathcal{E}}{1+\nu}\xi_{0,y}kl - \frac{d\mathcal{E}}{K^2(1-\nu^2)}\zeta_{0,yy}^2[(1-\nu)k^2 + 2l^2],$$

where $K^2 = k^2 + l^2$.

This has similar properties to the displacement relation (47) of §5.2.2. The first two terms arise from the flexural and hydrostatic terms respectively and are stabilizing. The third term arises from 'remaining' slack in the system, and can be destabilizing provided the solution for N_0 in the base state is negative. If N_0 is sufficiently large and positive (the system is very taut), then it may eliminate all instability. As in §5.2.2, the base state downstream stretching can be destabilizing and is responsible for symmetry breaking. Much more work must be done to complete this analysis.

6 Conclusions and future work

We have presented some preliminary analysis on an elastic-skinned gravity current and the wrinkling phenomenon that may be observed, under certain conditions, on the surface. This

wrinkling is most prominent due to a combination of a compressive pre-strain on the plate and fluid traction pulling at the base of the plate. The pulling is what is responsible for symmetry breaking. We have tried to remain consistent with the scalings under which the von Kármán plate equations hold. Some experimental observations have been explained from our analysis: the necessity of slack for wrinkles to be observed and the downstream orientation of the wrinkles.

There is still very much that can be done. The stability analyses can be completed in a WKB sense and can be considered numerically. Beyond that, quantitative experiments and numerical simulations using finite elements could be performed. Formulating boundary conditions for real elastic-skinned gravity currents should also be done.

7　Acknowledgements

References

[1] M. Clayton, Master's thesis, Penn State, 2004.

[2] C. D. Ollier, *Volcanoes* (MIT Press, Cambridge, MA, 1969).

[3] J. H. Fink and R. C. Fletcher, "Ropy pahoehoe: surface folding of a viscous liquid," J. Volcanol. Geoth. Res. **4**, 151 (1978).

[4] H. E. Huppert, "Flow and instability of a viscous gravity current down a slope," Nature **300**, 427 (1982).

[5] J. B. Grotberg and O. E. Jensen, "Biofluid mechanics in flexible tubes," Annu. Rev. Fluid Mech. **36**, 121 (2004).

[6] D. J. Gee, "Numerical continuation applied to panel flutter," Nonlinear Dynamics **22**, 271 (2000).

[7] T. B. Benjamin, "Effects of a flexible boundary on hydrodynamic stability," J. Fluid Mech. **9**, 513 (1960).

[8] A. Chakrabarti, D. S. Ahluwalia, and S. R. Manam, "Surface water waves involving a vertical barrier in the presence of an ice-cover," Int. J. Eng. Sci. **41**, 1145 (2003).

[9] N. J. Balmforth, R. V. Craster, and A. C. Rust, "Instability in flow through elastic conduits and volcanic tremor," J. Fluid Mech. (2004), submitted.

[10] A. E. Hosoi and L. Mahadevan, "Peeling, healing and bursting in a lubricated elastic sheet," Phys. Rev. Lett. (2004), to appear.

[11] Y.-Y. Yu, *Vibrations of elastic plates: linear and non-linear dynamical modelling of sandwiches, laminated composites, and piezoelectric layers* (Springer, New York, 1996).

[12] Y. C. Fung, *Foundations of solid mechanics* (Prentice-Hall, New Delhi, 1968).

[13] S. P. Timoshenko and S. Woinowsky-Krieger, *Theory of plates and shells* (McGraw-Hill, New York, 1959).

[14] L. D. Landau and E. M. Lifschitz, *Theory of elasticity* (Pergamon, Oxford, 1970).

[15] P. G. Ciarlet, "Une justification des équations de von Kármán," C. R. Acad. Sc. Paris Série A **288**, 469 (1979).

[16] O. Millet, A. Hamdouni, and A. Cimetière, "A classification of thin plate models by asymptotic expansion of non-linear three-dimensional equilibrium equations," Nonlinear Mechanics **36**, 165 (2001).

[17] S. S. Antman, *Nonlinear problems of elasticity* (Springer, New York, 1995).

[18] J. J. Stoker, *Nonlinear elasticity* (Nelson, London, 1968).

[19] R. Huang and Z. Suo, "Wrinkling of a compressed elastic film on a viscous layer," J. Appl. Phys. **91**, 1135 (2002).

[20] Y. W. Wong and S. Pellegrino, in *43rd AIAA/ASME/ASCE/AHS/ASC Structures, structural dynamics, and materials conference* (AIAA, Denver, CO, 2002).

[21] E. H. Mansfield, *The bending and stretching of plates*, *International series of monographs on aeronautics and astronautics* (Pergamon, Oxford, 1964).

[22] Y. W. Wong and S. Pellegrino, in *New approaches to structural mechanics, shells and biological structures*, edited by H. Drew and S. Pellegrino (Kluwer, Dordrecht, 2002), Chap. Amplitude of wrinkles in thin membrane.

[23] C. S. Riera, `http://people.deas.harvard.edu/~riera/drying.html`.